First-principles study of ultrafast magneto-optical switching in NiO

G. Lefkidis* and W. Hübner
Department of Physics, Kaiserslautern University of Technology, P.O. Box 3049, 67653 Kaiserslautern, Germany
(Received 4 May 2007; revised manuscript received 29 May 2007; published 12 July 2007)

We present a fully *ab initio* ultrafast magneto-optical switching mechanism in NiO. All intragap *d* states of the bulk and the (001) surface are obtained with highly correlational quantum chemistry and propagated in time under the influence of a static magnetic field and a laser pulse. We find that demagnetization and switching can be best achieved in a subpicosecond regime with *linearly* rather than *circularly* polarized light. Going beyond the electric dipole approximation is mandatory for the bulk and greatly enhances the process even for the surface, where it is not required by symmetry.

DOI: 10.1103/PhysRevB.76.014418 PACS number(s): 78.68.+m, 73.20.−r, 78.20.Ls, 78.47.+p

I. INTRODUCTION

The continuous miniaturization and speed upscaling of modern computers and magnetic recording media give rise to a constant strive to derive and optimize mechanisms in order to manipulate as fast as possible the magnetic moment of a material. Ever since the light induced demagnetization of ferromagnets was discovered,[1] several light-driven scenarios and mechanisms have been proposed,[2,3] and it has already been demonstrated that exploiting the ultrafast electron-photon interaction can lead to subpicosecond dynamics.[4] Magnetic dichroism and nonlinear magneto-optical Kerr experiments underline the necessity for quantitative spin-orbit coupling (SOC) calculations,[5,6] the latter interaction being a mandatory prerequisite for optical spin control, an important ingredient for future applications. Furthermore, it has been experimentally assessed that the electronic excitations can nonthermally control spin dynamics[7] and magnetic phases[8] in magnetic materials. In this paper, we present a detailed mechanism for the description of such a SOC-mediated switching scenario on a real material based exclusively on laser pulses where we (i) achieve all-optical magnetic switching on a purely *ab initio* level, (ii) switch both surface and bulk, and (iii) are able to include an additional external magnetic field.

In our calculations, we do not include any empirical parameters (unlike previous works in that field) and regard a realistic strongly correlated solid material rather than a simple atomistic model. The switching scenario presented here is a realization of what was previously suggested by Gómez-Abal *et al.*[4,9] Taking into account the importance of SOC effects and the subtleties of the scenario, it is more than necessary to investigate the theories on a realistic level and not only on the level of an "idea." Moreover, we differentiate between several switching mechanisms [electric dipoles (EDs) vs magnetic dipoles (MDs)] and investigate the importance of the magnetic field (again with no first-principles precedence in the literature to the best of the authors' knowledge). Finally, we present a recipe which relies solely on our specific quantum chemical calculations and the careful analysis of the switching results on the system.

NiO is a possible candidate for such a scenario, since it possesses the following main features: (i) dispersionless, explicitly addressable intragap states, (ii) SOC mixing, (iii) a well known crystallographic and magnetic structure, and (iv) simple phononic modes. As test systems, we choose two doubly embedded clusters, NiO_5^{-8} and NiO_6^{-10}, which represent the (001) surface and the bulk of NiO, respectively. The first embedding is a shell of effective core potentials which account for the Ni ions in the immediate vicinity of the oxygens and the second one is a charge point field ($15\times15\times15$ and $15\times15\times8$ for bulk and surface, respectively) which describes the Madelung potential. The intragap *d* states are computed with a high-level multiconfigurational complete active space (CAS) method[10] using the nonrelativistic GAUSSIAN03 code.[11]

II. THEORY

The Hamiltonian of the interacting system is solved in three steps. First, the static nonrelativistic Hamiltonian is solved with the complete active space method which incorporates both static and dynamical correlations in a self-consistent way:[10,12]

$$\hat{H}_{\mathrm{CAS}} = -\frac{1}{2}\sum_{i=1}^{N_{\mathrm{el}}}\nabla^2 - \sum_{i=1}^{N_{\mathrm{el}}}\sum_{a=1}^{N_{\mathrm{at}}}\frac{Z_a}{|\mathbf{R}_a-\mathbf{r}_i|} + \sum_{i=1}^{N_{\mathrm{el}}}\sum_{j=1}^{N_{\mathrm{el}}}\frac{1}{|\mathbf{r}_i-\mathbf{r}_j|} + \sum_{a=1}^{N_{\mathrm{at}}}\sum_{b=1}^{N_{\mathrm{at}}}\frac{Z_aZ_b}{|\mathbf{R}_a-\mathbf{R}_b|}. \quad (1)$$

N_{el} and N_{at} are the numbers of electrons and atoms, respectively, $\mathbf{r}_i$ and $\mathbf{R}_\alpha$ the position vectors of the electrons and the atoms, and Z_α the charges of the nuclei. Then, SOC and the static external magnetic field $\mathbf{B}_{\mathrm{stat}}$ are turned on by diagonalizing $\hat{H}^{(1)}$ on the basis of the many-body wave functions obtained by $\hat{H}_{\mathrm{CAS}}$:

$$\hat{H}^{(1)} = +\sum_{i=1}^{N_{\mathrm{el}}}\frac{Z_a^{\mathrm{eff}}}{2c^2R_i^3}\hat{\mathbf{L}}\cdot\hat{\mathbf{S}} + \sum_{i=1}^{N_{\mathrm{el}}}\mu_L\hat{\mathbf{L}}\cdot\mathbf{B}_{\mathrm{stat}} + \sum_{i=1}^{N_{\mathrm{el}}}\mu_S\hat{\mathbf{S}}\cdot\mathbf{B}_{\mathrm{stat}}. \quad (2)$$

$\hat{H}_{\mathrm{CAS}}$ and the first term of $\hat{H}^{(1)}$ represent the material properties. SOC is computed by means of the one-electron Breit operator where effective nuclear charges (Z_a^{eff}) account for the two-electron terms.[13] The other terms of $\hat{H}^{(1)}$ denote the interaction with the external static magnetic field, with $\hat{\mathbf{L}}$ and $\hat{\mathbf{S}}$ being the orbital and spin momentum operators, respec-

tively (we keep only terms linear in $\mathbf{B}_{\text{stat}}$), μ_L and μ_S their respective gyromagnetic ratios, and c the speed of light. Finally, the obtained static magnetic states are propagated in time under the interaction with a suitably tailored laser field:

$$\hat{H}^{(2)} = \mathbf{p}^{(\text{CAS}+1)} \cdot \mathbf{A}_{\text{laser}}(t) + \hat{\mathbf{S}} \cdot \mathbf{B}_{\text{laser}}(t). \tag{3}$$

$\mathbf{p}^{(\text{CAS}+1)}$ is the electron momentum as calculated in the second step and $\mathbf{A}_{\text{laser}}(t)$ and $\mathbf{B}_{\text{laser}}$ are the time-dependent vector potential and magnetic field of the laser pulse, which is treated classically. For this step, time-dependent perturbation theory is applied. All terms can be switched on and off at will, thus giving an estimate of their importance in the process. In the bulk, SOC splits the first excited state ($^3T_{2g}$) into four groups (E_g, T_{1g} with $\Delta E \approx 18$ meV, T_{2g} with $\Delta E \approx 69$ meV, and A_{1g} with $\Delta E \approx 87$ meV). Since all of them retain their *gerade* character, the transition from and to the ground state (A_g) is still ED forbidden. Thus, MD transitions have to be taken into account.[12,14] Our SOC splittings are slightly larger than the values given by Satitkovitchai *et al.*,[15] who, using the COLUMBUS code and the configuration interaction with single excitations method, give very high energy values for these states (1.02 eV compared to 0.94 eV in the present work). Both results do not take into account further splittings due to intersite spin-spin interactions and the ⟨111⟩ distortion. Experiment shows several peaks between 0.96 and 1.04 eV.[14]

All states are propagated in the interaction picture

$$\frac{\partial c_\alpha(t)}{\partial t} = \frac{-i}{\hbar} \sum_\beta \langle \alpha | \hat{V}(t) | \beta \rangle c_\beta(t) e^{-i(E_\beta - E_\alpha)t/\hbar}, \tag{4}$$

where $|\alpha\rangle$ and $|\beta\rangle$ are the unperturbed eigenstates, c_α is the complex scalar coefficient of state α in the wave function $\Psi(t) = \Sigma c_\alpha(t) e^{-iE_a t/\hbar} |\alpha\rangle$, E_α is the energy of state α, and $\hat{V}(t)$ is the perturbation operator [laser field as given in Eq. (3)]. We integrate over time the coupled differential equations [Eq. (4)] using the fifth order Runge-Kutta method combined with the Cash-Karp adaptive step size control with a convergence threshold of 10^{-6} for the normalization condition. Stricter thresholds, while computationally extremely costly, proved to be not necessary. Before every pulse, a starting point is considered where a single ground state (either the "spin-up" or "spin-down" ground state) is fully populated. From our *ab initio* calculations for NiO, we achieve a repeatability of more than ten duty cycles and a population fidelity of ~98% after 10 cycles. The "lost" population remains mainly in the excited states and not the initial ground state; thus, slow (thermal) relaxation effects would lead the system to an almost perfect switch. Repeated pulses do not increasingly deteriorate the process quality, at least not until a big percentage of the population gets transferred to higher excited states (after about 15–20 cycles, depending on the laser intensity).

III. RESULTS

First we must find which excited states are involved in the process. It was already shown that for a Λ process (see inset in Fig. 1), at least four levels are required,[9] i.e., (i) two ground states with spin up and spin down, respectively, and (ii) two excited states with spin up and spin down mingled by a spin-mixing mechanism (SOC and/or magnetic field) to generate at least one nonpure spin state, accessible from both ground states. In the absence of external magnetic fields, the three spin states of a triplet ($S_z = 1, -1$, and 0) are degenerate and all their linear combinations are valid solutions to the Schrödinger equation. Thus, if the system is in the ground state and in thermal equilibrium, all three of them are equally populated and $\langle S_z \rangle$ averages to zero. Furthermore, one can rotate the many-electron wave function in that triplet subspace, making the choice of spin up and spin down arbitrary. However, even an infinitesimal field suffices to lift these degeneracies (Zeeman effect), resulting in nonzero $\langle S_z \rangle$ values. So, for the bulk of NiO, which possesses octahedral symmetry (equivalent to spherical), the spins are always parallel (or antiparallel) to the applied field, and their magnitude depends on the field strength. While the Zeeman energy shiftings do not depend on the choice of the axis, the magnetic moment projections do. This is not the case for the surface of NiO, where the spatial symmetry can induce a spin direction as well. If, however, the external field gets strong enough, it can force spins to align with it.[16] Generally, in the presence of the crystal field, $\langle L_z \rangle$ may get quenched due to lack of rotational invariance around the z axis. Of course, the inclusion of SOC in the Hamiltonian leads to S_z not being a good quantum number. Still, one can compute $\langle S_z \rangle$ and quite often gets approximately ±1 or 0, an almost pure spin state. This is yet the case for both our clusters, since ground and excited states are energetically well separated, an advantage exclusive to dispersionless systems such as NiO. Note that SOC alone cannot always specify a direction for the spins. Although the

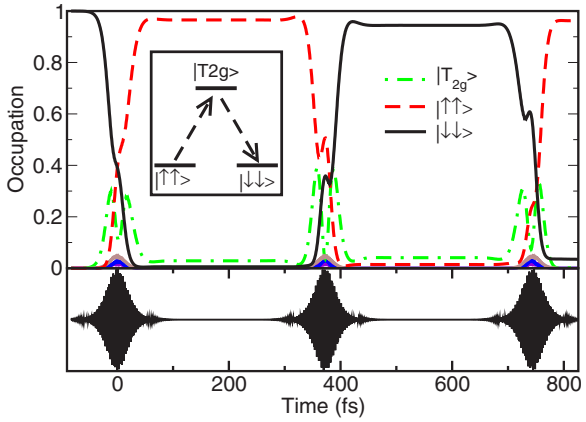

FIG. 1. (Color online) Top: population evolution of the lowest lying levels in bulk of NiO. The solid black line and the red (dark gray) dashed line show the occupations of the spin-up and spin-down states, respectively. The Λ process is achieved through one spin-mixed excited state [dashed green (light gray) line], namely, E_g (T_{2g} before SOC splitting), and always gets twice populated and depopulated during the laser pulse. The population transfer is completed in about 100 fs. The polarization is linear and perpendicular to the externally applied static magnetic field $B_{\text{ext}} = 12.5$ A/m. Bottom: laser profile. The pulse has FWHM of 140 fs, energy of 0.9166 eV, and B_{max} of 125 000 A/m. Inset: Λ process (schematic).

TABLE I. Energies, symmetries (after SOC), and total angular momenta of the 12 lowest states for the NiO_5^{-8} and NiO_6^{-10} clusters. States marked bold can be used for switching. For the bulk, states 1 and 3 are considered spin up and spin down, and states 2 and 3 for the surface states (in both cases, the energy differences are minimal).

	Bulk			Surface		
State	Symmetry	Energy (eV)	$\langle J_z \rangle$	Symmetry	Energy (eV)	$\langle J_z \rangle$
12	$1A_{1g}$	0.9674	**0.00**	$3E$	0.9256	0.69
11	$1T_{2g}$	0.9551	0.68		0.9256	−0.69
10		**0.9551**	**0.00**	$2B_1$	0.9076	0.00[a]
9		0.9551	−0.68	$2B_2$	**0.5795**	**0.00**
8	$2T_{1g}$	0.9248	0.60	$1B_1$	**0.5570**	**0.00**
7		**0.9248**	**0.00**	$2E$	0.5162	1.28
6		0.9248	−0.60		0.5162	−1.28
5	$1E_g$	**0.9166**	**0.00**	$1A_2$	**0.4480**	**0.01**
4		**0.9166**	**0.00**	$1A_1$	**0.4372**	**−0.01**
3	$1T_{1g}$	0.0000	1.20	$1E$	0.0032	1.31
2		0.0000	0.00		0.0032	−1.31
1		0.0000	−1.20	$1B_2$	0.0000	0.00

[a]The state has $\langle J_z \rangle = 0$ but originates (before SOC splitting) from an $^3A_2$ state for which the transition from the ground state is forbidden by symmetry (Ref. 10).

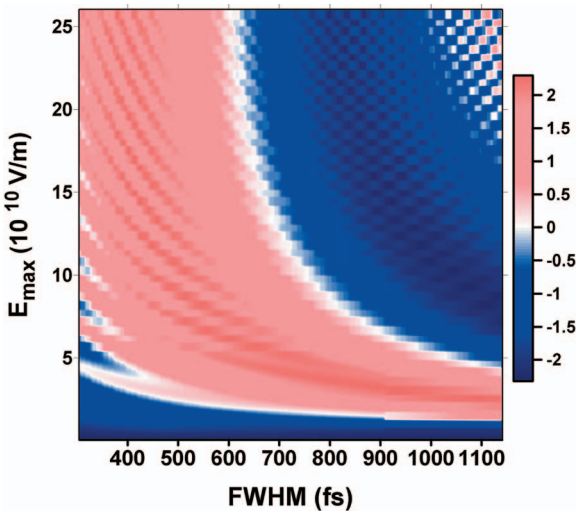

FIG. 2. (Color online) Perpendicular magnetic field. Contour plot of the magnetic state of the NiO_5^{-8} cluster after the application of a linearly polarized sech^2-shaped laser pulse and an external static magnetic field $B_{ext}=B_z=12.5$ A/m vs duration and intensity of the pulse. Calculations are done within the ED approximation. The first excited state $[1A_1^{(\uparrow\downarrow)}$ at $E=0.4372$ eV] is chosen as the intermediate state. Colors indicate the total angular momentum after the pulse. The magnetization before the pulse is 1.31 a.u.. The red (light gray) area means switching is achieved. Several combinations of pulse duration and strength can lead to magnetization reversal (crossing the white border line where the magnetization is zero).

antiferromagnetic (AF) ordering in NiO (both bulk and surface) cannot be accounted for in our single-site model, the local magnetic moment is not expected to differ much.[17] Note as well that NiO exhibits high spin density only on the Ni sites, thus justifying our local picture.

Second, we fully populate the spin-up ground state (see Table I) and propagate in time while applying a finite external sech^2-shaped laser pulse with systematically varied intensity, duration, and angle of incidence of the laser pulse. The task to achieve switching amounts to choosing a suitable mixed-spin excited state. We find the maximum efficiency when the matrix elements from both ground states have approximately the same absolute values. The relative phase of the light and the wave function turns out not to affect the process, since no appreciable population transfer takes place until the phases match. However, the phase evolution of the different states governs the direction of the population transfer during the pulse. So the intermediate excited state(s) typically exhibit(s) a double peak during the process (see Fig. 1).

The simple $|E| \cdot \text{FWHM} = \text{const}$ (FWHM denotes full width at half maximum), rule of thumb as seen in the model calculations of Gómez-Abal *et al.* (see Ref. 9, Fig. 5), is reproduced only for pulses longer than about 500 fs, while shorter ones generate a more complex behavior. For the bulk calculation, we include MD matrix elements, since it was already shown that they are responsible for the transitions from the ground to the intragap *d*-character states,[10,14] unless phonons and/or lattice distortions are taken into account. These would, in fact, enhance even more the process, since their presence facilitates electronic transitions.[12]

Even with very intense pulses, it was not possible to depopulate the original state in one step because the population transfer depends not only on the population difference but on the relative phases as well, and some time passes before the intermediate excited state gets in phase with the target ground state so that the population flows toward the latter one and not toward the initial ground state. An extremely intense pulse could circumvent this at the cost of uncontrolled off-resonance electron excitations. In principle, it is possible to achieve both demagnetization and switching with a variety of pulses. Figure 2 shows the dependence of the spin magnetic moment of the NiO(001) surface after the pulse with respect to its duration and intensity. The static *B* field is *perpendicular to the surface* and the laser pulse is *linearly* polarized at a direction parallel to the surface. Contrary to previous works,[4,9] we do not find optimal switching conditions for circularly but for linearly polarized light, more specifically, with propagation direction parallel to the static *B* field—this is consistent with the experimental findings of Koopmans *et al.* in an experimental setup similar to ours (almost normal incidence and sensitivity to the out-of-plane magnetization component) that the demagnetization time of Ni thin films is not affected by pump helicity.[18] Our calculations indicate that the use of circularly polarized light can selectively activate one channel of the Λ process, allowing only either excitation or de-excitation (resembling Rabi oscillations), while a superposition of the two polarizations can selectively control the percentage of the population transfer. In the case of *circularly* polarized light, one transition can be up to twice as effective as in the case of linearly polarized

light; however, the other transition is then blocked. By *tilting* the direction of the propagation of the light with respect to the static B field, one can overcome this selectivity. For example, with an external field perpendicular to the (001) surface and a propagation direction parallel to the surface, switching is possible with all polarizations, however, the $E_{\max}$ of the pulse needed is about 1 order of magnitude bigger. This finding was obscured in Ref. 4 by the absence of the external magnetic field in the calculations, thus making the choice of spin up and spin down arbitrary and any of their linear combinations a valid eigenfunction for the ground state. Demagnetization of the system (choosing $\langle J_z \rangle \approx 0$ as final ground state in Table I) is also possible and best achieved for linearly polarized light at an angle of 45° with respect to the magnetic field. However, it is generally less efficient than switching. Moreover, the $\langle J_z \rangle \approx 0$ state is metastable and the spin-spin interactions will convert it to an unpredictable AF domain.

IV. DISCUSSION

Our calculations indicate that the laser interacts with the electrons mainly through the $\mathbf{p}^{(\mathrm{CAS}+1)} \cdot \mathbf{A}_{\mathrm{laser}}(t)$ term. Although L_z is not a good quantum number in the presence of SOC, the field must basically couple to the orbital rather then the spin angular momentum for it is the product of the two transition probabilities that governs the Λ process. So (irrespective of whether one restricts oneself to the ED approximation), it is the orbital angular momentum of the electronic state that needs to be changed by the light, turning the Λ process to two consecutive additions (or subtractions) of angular momentum (the pulse can of course couple to the spin and flip it directly—*not* a Λ process—but more slowly and at the far infrared region). Since, however, one transition is an absorption and the other an emission of a photon, the helicities of the two photons must differ, making linearly polarized light the obvious choice if one wants to have both transitions driven by the same pulse. Thus, the recipe to achieve switching (using ED for the surface and MD for the bulk) is to find an excited state with $\langle L_z \rangle \approx 0$. Furthermore, the chosen state needs to originate from a state with a symmetry that does not forbid transition matrix elements, otherwise, even though the lowering of the symmetry due to SOC and B_{ext} may make the transition possible, the elements will be of very small magnitude.

So, for the *surface* (within the ED approximation), the best results were achieved with the $1E_g^{(\uparrow\uparrow)} \leftrightarrow 1A_1^{(\uparrow\downarrow)} \leftrightarrow 1E_g^{(\downarrow\downarrow)}$ process (the parentheses in the superscripts indicate the fact that S_z is not really a good quantum number). If we use the symmetry labels before the addition of the SOC splitting, namely, $1\,{}^3B_1^{\uparrow\uparrow} \leftrightarrow 1\,{}^3E^{\uparrow\downarrow} \leftrightarrow 1\,{}^3B_1^{\downarrow\downarrow}$, we immediately recognize the ED allowed $E \leftrightarrow B_1$ transition.

Regardless of the inclusion or not of SOC in our calculations, both the ground and *all* the intragap states of the *bulk* are of gerade symmetry (see Table I), making the transitions among them forbidden. Within the ED approximation, this can only be overcome by the use of charge transfer states as intermediate ones, however, this results in having to deal with wide bands instead of dispersionless states, which cannot be as easily and as explicitly addressed. Note that generic spin dynamics always results from electronic correlations, and as such, requires narrow bands. If, however, one includes MD transitions, then the dispersionless intragap states are perfectly accessible, a fact seen both in linear and nonlinear optics.[14] So, the best results were achieved via the $1T_{1g}^{(\uparrow\uparrow)} \leftrightarrow 1E_g^{(\uparrow\downarrow)} \leftrightarrow 1T_{1g}^{(\downarrow\downarrow)}$ process. Using again the symmetry labels before the SOC splitting $(1\,{}^3A_{2g}^{\uparrow\uparrow} \leftrightarrow 1\,{}^3T_{2g}^{\uparrow\downarrow} \leftrightarrow 1\,{}^3A_{2g}^{\downarrow\downarrow})$, we recognize the transition $A_{2g} \leftrightarrow T_{2g}$ which is ED forbidden but MD allowed.

If we additionally include MD transitions in our surface calculations we see a dramatic change, a fact that was expected from several previous works.[10,19] Atomistically, the origin of this is not the tremendous efficiency of the MD transitions but rather the small values of the ED transition elements. The intragap states consist mainly of Ni d orbitals, so the transition elements between them, although allowed by symmetry, are very weak. Thus, the main contributions arise from admixtures of virtual p-like excitations, turning high-level correlations to a *sine qua non* prerequisite for the separation of spin and charge dynamics. When including spin interactions not only via SOC but also explicitly by going

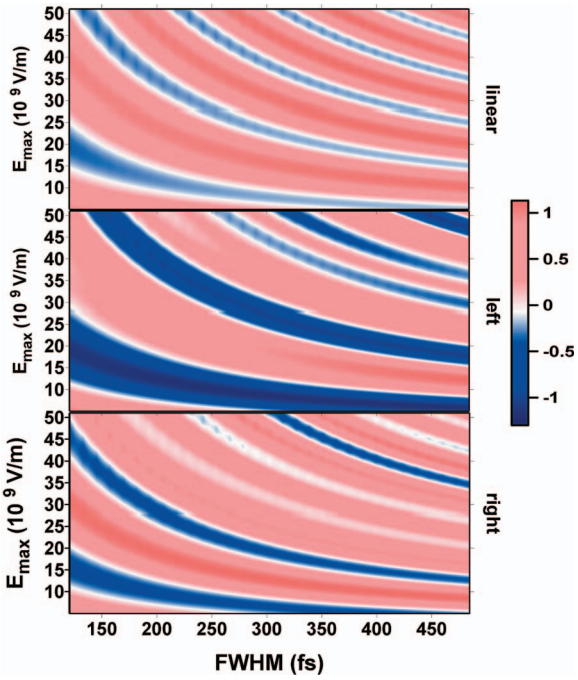

FIG. 3. (Color online) Tilted magnetic field. Contour plot of the magnetic state of the NiO_5^{-8} cluster after the application of a sech^2-shaped laser pulse and an external static magnetic field $B_{\mathrm{ext}} = 12.5$ A/m tilted by 60° from the perpendicular direction vs duration and intensity of the pulse. Calculations are done within the ED approximation and the first excited state $[1A_1^{(\uparrow\downarrow)}$ at $E=0.4372$ eV$]$ is chosen as the intermediate state. The polarization of the light is s linear (up), left circular (middle), and right circular (bottom). Colors indicate the total angular momentum after the pulse. The magnetization before the pulse is 1.31 a.u.. The red (light gray) area means switching is achieved. Several combinations of pulse duration and strength can lead to magnetization reversal (crossing the white border line where the magnetization is zero). Note, however, that the combinations vary for different polarizations.

beyond the ED approximation, we can practically switch for many given polarizations, ellipticities, and geometries. Note that (i) it is possible to find combinations of pulse strength and duration where only one polarization can switch or demagnetize and (ii) one switches best (not only marginal change of sign but large magnetic moment) with left polarized light, where the MD and ED transitions act synergetically (see Fig. 3).

Note that despite the linear polarization of the pump pulse, the electromagnetic field still acts as a reservoir for the angular momentum in the model,[20] a direct consequence of angular momentum conservation and selection rules. In an experiment, this would be observed by measuring the polarization and ellipticity of the reflected (or transmitted) light. In our semiclassical calculations, however, we are unable to account for spontaneous emission and the feedback of angular momentum to the pump pulse.

In all the presented calculations, we always start from a single occupied state, and the results indicate that the relative phase of matter and light does not influence the outcome. If the system, however, is initially prepared in a superposition of states, then their relative phases induce quantum interference patterns. The same holds for two-pulse scenarios for the phases of the electromagnetic fields.[21] Note also that even elevated temperatures do not affect the localized electronic distribution, since we are dealing with an insulating material (see also discussion in Ref. 12, Appendixes B and C).

V. CONCLUSION

In conclusion, we presented an ultrafast magneto-optical switching scenario based entirely on *ab initio* calculations for both the bulk and the (001) surface of NiO. We showed that controlled switching is possible by including SOC in order to take advantage of a Λ process. Furthermore, we showed the necessity of including a static magnetic field in order to distinguish spin-up and spin-down states and the importance of including MD transitions in order to realize the Λ process in the centrosymmetric bulk. All these ideas were combined together in a realistic material, with no empirical parameters. So several scenarios were investigated using the laser and the static magnetic field as freely tunable parameters in a way to gain full control and maximum efficiency of the process.

ACKNOWLEDGMENTS

We would like to acknowledge support from the European DYNAMICS Research Training Network, the MINAS Landesschwerpunkt, and Priority Programmes 1133 and 1153 of the German Research Foundation.

*lefkidis@physik.uni-kl.de

[1] E. Beaurepaire, J.-C. Merle, A. Daunois, and J.-Y. Bigot, Phys. Rev. Lett. **76**, 4250 (1996).
[2] B. Koopmans, J. J. M. Ruigrok, F. Dalla Longa, and W. J. M. de Jonge, Phys. Rev. Lett. **95**, 267207 (2005).
[3] J. Chovan, E. G. Kavousanaki, and I. E. Perakis, Phys. Rev. Lett. **96**, 057402 (2006).
[4] R. Gómez-Abal, O. Ney, K. Satitkovitchai, and W. Hübner, Phys. Rev. Lett. **92**, 227402 (2004).
[5] S. Altieri, M. Finazzi, H. H. Hsieh, H. J. Lin, C. T. Chen, T. Hibma, S. Valeri, and G. A. Sawatzky, Phys. Rev. Lett. **91**, 137201 (2003).
[6] B. Koopmans, M. van Kampen, J. T. Kohlhepp, and W. J. M. de Jonge, Phys. Rev. Lett. **85**, 844 (2000).
[7] A. V. Kimel, A. Kirilyuk, P. A. Usachev, R. V. Pisarev, A. M. Balashov, and T. Rasing, Nature (London) **435**, 6558 (2005).
[8] T. Lottermoser, T. Lonkai, U. Amann, D. Hohlwein, J. Ihringer, and M. Fiebig, Nature (London) **430**, 541 (2004).
[9] R. Gómez-Abal and W. Hübner, Phys. Rev. B **65**, 195114 (2002).
[10] G. Lefkidis and W. Hübner, Phys. Rev. Lett. **95**, 077401 (2005).
[11] J. A. Pople *et al.*, GAUSSIAN 03, Revision B1, 2003.
[12] G. Lefkidis and W. Hübner, Phys. Rev. B **74**, 155106 (2006).
[13] S. Koseki, M. W. Schmidt, and M. S. Gordon, J. Phys. Chem. A **102**, 10430 (1998).
[14] M. Fiebig, D. Fröhlich, T. Lottermoser, V. V. Pavlov, R. V. Pisarev, and H.-J. Weber, Phys. Rev. Lett. **87**, 137202 (2001).
[15] K. Satitkovitchai, Y. Pavlyukh, and W. Hübner, Phys. Rev. B **72**, 045116 (2005).
[16] P. J. Jensen and H. Dreyssé, Phys. Rev. B **66**, 220407(R) (2002).
[17] X. Ren, I. Leonov, G. Keller, M. Kollar, I. Nekrasov, and D. Vollhardt, Phys. Rev. B **74**, 195114 (2006).
[18] F. D. Longa, C. J. T. Kohlhepp, W. J. M. de Jonge, and B. Koopmans, arXiv:cond-mat/0609698 (2006).
[19] E. B. Graham and R. E. Raab, Phys. Rev. B **62**, 9561 (2000).
[20] G. P. Zhang and W. Hübner, Phys. Rev. Lett. **85**, 3025 (2000).
[21] G. Lefkidis and W. Hübner (unpublished).